OBSERVATIONAL RESULTS ON THE INFLUENCE OF STABILITY AND WIND-WAVE COUPLING ON MOMENTUM TRANSFER AND TURBULENT FLUCTUATIONS OVER OCEAN WAVES

K. L. DAVIDSON
Dept. of Meteorology, Naval Postgraduate School, Monterey, California

(Received in final form 19 September, 1973)

Abstract. Turbulence data obtained over ocean waves during the BOMEX experiment of 1969 are presented. Procedures in measurement and analyses are described which include adjustments for possible platform, *R/V* FLIP, motion. Momentum transfer is shown to have been influenced by both stability and wind-wave coupling. The wind-wave coupling influence is separated from the stability influence and is described in terms of a linear dependence of the deviation from the logarithmic profile on C/u_*, where C is the phase speed corresponding to the wave spectrum peak. As observed by others, a value of C/u_* near 25 is associated with minimal wind-wave coupling influence. For C/u_* greater than 25, momentum transfer is decreased relative to the neutral profile prediction. Expressions are also presented for the wind-wave coupling influence on relative intensities, σ_u/u_*, σ_v/u_*, and σ_w/u_*. Values of the relative intensities approximate neutral overland values when the expressions are written such that the wave influence is zero near a C/u_* value of 25.

1. Introduction

University of Michigan personnel made a series of turbulence and wave measurements during the last two weeks of May 1969 in the Barbados Oceanographic and Meteorological Experiment (BOMEX). The measurements were made about 200 miles east northeast of Barbados (in the vicinity of 14°N latitude, 57°W longitude) from the Scripps Institution of Oceanography Floating Instrument Platform (FLIP).

The experiment had two purposes. First, it was desired to make direct measurements of the vertical turbulent fluxes of momentum and sensible heat for assimilation in the BOMEX core experiment. The core experiment has been described by Holland (1972). Second, it was desired to study the nature of the turbulent fluctuations and fluxes adjacent to the waves to determine the influence, if any, that the waves may have on them. For the latter purpose, existing results on both wind-wave coupling and stability influences were heavily relied upon for guidelines in interpretations.

The scope of the interpretations was to compare the observed fluxes and intensity of the fluctuations with predicted relationships which depend on scaling parameters for stability, Z/L and wind-wave coupling, C/u_*.

Methods for describing and interpreting the observational data were chosen deliberately to be similar to previous descriptions of BOMEX results as well as to other over-water turbulence results. Two BOMEX related papers of primary relevance are those by Paulson *et al.* (1972) and Pond *et al.* (1971). Measurements discussed in both

Boundary-Layer Meteorology **6** (1974) 305–331.

of these papers were made from FLIP during the two weeks immediately preceding our measurements. Other over-water turbulence results which provided considerable direction in the interpretation were those by Volkov (1969, 1970) and Kitaigorodskii (1969).

2. Measurements and Recording

2.1. Velocity measurements

Wind-velocity measurements were made with constant temperature hot-film anemometer systems with linearizers. The hot-film sensors were glass cylinders, 0.15 mm in diameter and 7.0 mm long, covered with conducting platinum films onto which quartz coatings were applied. Each anemometer probe had three mutually perpendicular sensors, making it possible to determine instantaneous three-dimensional wind vectors. The frequency response of the sensors was about 50 Hz.

The hot-film sensors appeared to perform satisfactorily in the salt air environment. Their performance was monitored closely during the two-week experimental period and in general, sensors used during any experimental period were exposed to the airflow less than 8 h and were operated less than 5 h between calibrations. A 10% decrease in sensitivity (27 m s^{-1} indicated in a 30 m s^{-1} flow-rate calibration test) was the largest observed for several sensors which had been exposed to the airflow for over 36 h.

2.2. Temperature measurements

Air-temperature fluctuations were measured with a fine resistance wire (30 Ω tungsten filament, 0.0038 mm in diameter, 55 mm long) operated in a Wheatstone bridge with a filament current of about 2 mA. An output of 125 mV from the system corresponded to about 1°C change. In laboratory tests with a constant temperature and various filament resistances to simulate temperature changes, the filament and bridge were found to be capable of resolving temperature fluctuations of 0.05°C. The temperature sensors were mounted about 5 cm above the velocity sensors.

2.3. Wave measurements

Wave data were obtained from a resistance wave gauge*, consisting of a nonconducting tube, approximately 2.5 cm in diameter with a conducting wire wrapped spirally around it.

2.4. Mounting arrangements and platform consideration

Sensors for turbulence and profile measurements were mounted on a vertical mast, supported by a horizontal boom, about 15 m crosswind from FLIP's hull. The arrangement is shown in Figure 1. All sensors were vertically aligned and positioned approximately 1.5 m windward from the vertical mast. Sensors for velocity and temperature-fluctuation measurements could be located at 2, 3, 6, and 8 m above the water. Simul-

* Wave height data were measured by Dr R. E. Davis of Scripps Institution of Oceanography who allowed University of Michigan personnel to record them.

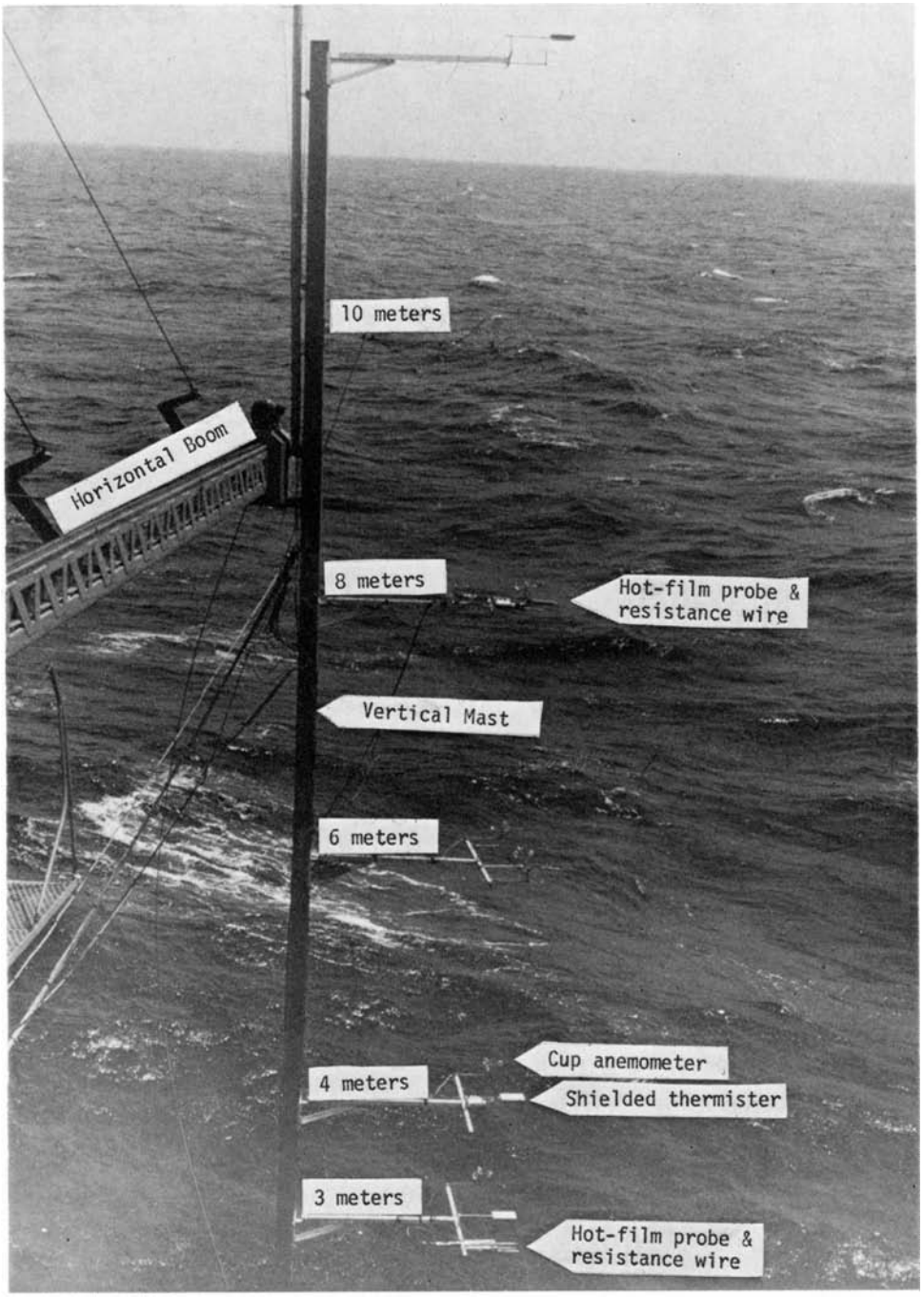

Fig. 1. Sensor mounting arrangment on the *R/V* FLIP.

taneous measurements at two levels were made in several observation periods; they appear at both 3 and 8 m in Figure 1. Mean wind and temperature measurements were made at 2, 3, 4, 6, 8, 12, and 16 m and have been presented by Superior (1970). The wave sensor was attached to the horizontal boom about 5 m inboard from the vertical mast.

Sensor mounting provision on FLIP and procedures for keeping FLIP oriented with respect to the wind direction have been described by others who made turbulence and profile measurements from FLIP during BOMEX, e.g., Paulson *et al.* (1972) and Pond *et al.* (1971). FLIP's orientation with respect to wind direction was maintained by a line to an attending tug, the SALISH, which was positioned downwind about 800 m. Oscillations of FLIP associated with this orientation procedure have not been described quantitatively and probably cannot be. Unfortunately, no provisions were available for adjusting the orientation of the vertical mast, independent of FLIP's orientation. This made it impossible to maintain sensors in a fixed level position and correction procedures during analyses have differed among investigators.

Wind-field distortion by the super-structure of FLIP was examined before the experiment in wind-tunnel model tests by Mollo-Christensen (1968). With the configuration used during BOMEX (Run 35, page 24), a maximum wind-speed error of 3% at a scale distance of 11.4 m from the model hull was found. This maximum error occurred at a scale height of 5 m, with lower errors at the heights we used for measurements. After Mollo-Christensen's work, the side boom on FLIP was lengthened from 11.4 m to 15 m to decrease further any wind-speed errors.

2.5. Recording

Velocity, temperature and wave measurements were recorded simultaneously on two seven-channel FM analog magnetic tape recorders (Ampex SP-300). Before the signals were recorded, a DC portion was suppressed with a known and constant opposing voltage, and the remaining signal was amplified. Knowledge of the suppressed DC levels enabled later determination of the three-dimensional wind vector sensed by the hot-film probe. The recordings were synchronized with a 300-Hz sine wave supplied to one channel of each recorder. Each recording period lasted about 80 min, a duration that was determined by the amount of tape on a reel.

3. Data Processing Procedures

In the following paragraphs descriptions are given of the procedures used to calculate velocity components and their zero-lag statistics and spectral estimates. Zero-lag statistics computed for each velocity component were its mean, variance, skewness, kurtosis and the covariances formed by pairing it with each of the other components. The processing included a method to adjust variance and covariances to compensate for the motion of FLIP. The adjustment is not an exact correction for the possible errors due to FLIP motion but is thought to be the best that can be made with the available information.

3.1. Digitizing

The signals were digitized at a sampling rate of 50 points s^{-1} in conjunction with analog low-pass filtering having a cut-off at 12.5 Hz. Signals that were recorded simultaneously were digitized in parallel using identical filters. Corrections for recorder gain and drift during the recording, determined by calibration during each period, were also performed at this stage. The digital records were further reduced to records of 25 points s^{-1} with a numerical 5-weight inverse transform smoothing function which had 7 Hz cut-off and 12 Hz terminal frequencies. Each record was 10.9 min long and had 16, 384 data points.

3.2. Calculation of velocity components

The desired coordinate system for interpreting velocity fluctuations is one with an axis parallel to the mean horizontal wind, an axis transverse in the horizontal and an axis transverse in the vertical. These define, respectively, the orthogonal velocity components, u, v, and w. Such components were obtained from the three orthogonal components measured by the probe in an arbitrary orientation through a transformation by rotation of axes. For the rotation, direction cosines had to be determined between the axes in the desired coordinate system and the axes in the one defined by the probe. Three sets of three-direction cosines are required, but because of the relations $\sum_{i=1}^{3} \cos^2\theta_i = 1$, only two of the three sets had to be determined.

The set of three direction cosines defining the along-wind axis with respect to the probe are given directly by those angles that the vector mean wind makes with the sensors. A second set of three direction cosines was obtained by assuming that the mean wind, averaged over a long enough period, changed direction only in the horizontal plane. With this assumption, the direction cosines defining the horizontal plane are obtained from the cross-product of two separate mean wind vectors. To explore the reliability of the scheme, a sample record was treated with averaging periods ranging from 41 s to 22 min and surprisingly consistent direction cosines were obtained between all averaging periods. It appeared sufficient, consequently, to use two consecutive 22-min periods to form averages from which direction cosines were computed with the cross-product technique.

This method may be compared to that used by Pond *et al.* (1971) who forced the average of the ratio,

$$\Phi_{uw}/(\Phi_u \Phi_w)^{1/2} \tag{1}$$

from spectral estimates at low frequencies, to equal -0.5 in the spectral band $0.01 < (fz/u) < 0.1$. Such a method would be needed if total velocity components were not recorded. Because of previously noted changes in the hot-film sensitivities over extended measurement periods, computed velocities were further scaled to agree with coincident cup anenometer observations by Superior (1969). The latter were made at several levels at the same time as our hot-film measurements and both short- and long-period mean values were available from cup counter readings taken at 10- to

15-min intervals. Hence, mean cup results were available for shorter periods than those reported by Superior (1969). The scaling was such that the hot-film mean horizontal wind speeds coincided with the cup mean wind speeds.

3.3. Calculations of zero-lag statistics and spectra

Before zero-lag statistics and spectra were calculated, each record was edited to remove erroneous data points which could have been due to a number of causes in the recording procedures. Data points were judged to be erroneous, and replaced by interpolated values, if their differences from the mean exceeded four times the initial standard deviation calculated for the 10.9 min period. Interpolated values were determined from the average of the two adjacent non-rejected values in the record. Further adjustments were made to variance and covariance values based on the computed means for the v and w components. Because direction cosines used in initial component determinations were based on averages for 22-min periods, $\bar{v}$ and $\bar{w}$ were not necessarily zero for individual 10.9 min periods; $\bar{w}$ and $\bar{v}$ for each period were therefore forced to zero using coordinate rotation and then the variance and covariance values were recalculated.

Spectral estimates were calculated for records to which had been applied, in addition to the above editing procedures, (1) a least-squares linear regression to remove the trend and (2) a cosine bell filter to remove unwanted end effects due to the finite sampling lengths (Oort and Taylor, 1969). A fast-Fourier transform algorithm was used to obtain coefficients for computing variance and covariance spectral estimates. The number of estimates was reduced from 8192 harmonics, resulting from a transform on 16384 points, to 93 by averaging together neighboring estimates. The averaging method, also described by Oort and Taylor (1969), was one in which the number of estimates averaged together increased logarithmically with frequency.

3.4. Adjustments for flip motion

Pitch and roll motions of FLIP introduced energy in the velocity spectra at the frequency corresponding to the swell frequency. Adequate measurements to correct the data for this motion were not made. Spectra of the motions, however, have been observed to approximate closely the shape of wave spectra. Zero-lag statistics were recalculated with adjustment for this possible platform motion even though wave related motion in the airflow is possible at the reported measurement levels. These additional estimates in conjunction with those obtained with no adjustment for FLIP's possible motion should describe the envelope for the most probable estimate of the statistics.

Adjusted zero-lag statistics were obtained by multiplying each by the ratio of the integrated variance or covariance spectra before and after extrema coincident with the wave spectra peak were removed. Linear interpolations between points adjacent to the bands associated with the extrema were used in the removal. Extrema removal and integrations were performed numerically, but frequency bands associated with the extrema were determined on the basis of visual examination of spectra.

The narrowness of the extrema bands supports a linear interpolation procedure for removing the extrema. Interpolations were applied to the identical bands for all

variables in a 10.9-min period. Furthermore, the extrema bands were very consistent over entire 77-min measurement periods.

Average adjustments for u_*, σ_u, σ_v, and σ_w were 8.2, -11.4, -8.3, and -4.0% respectively. In comparison, Pond *et al.* (1971) observed 5 to 10% differences between spectral integrals with and without these extrema removed. Our spectral integral differences for $\overline{uw}$, $\bar{u}^2$, v^2, and $\bar{w}^2$ based on the above values are 17, -20, -16, and 7% respectively.

Adjustments were not made to σ_T or $\overline{wT}$ results since adjustments computed for several periods were found to be less than 1%.

4. Observations and Results

4.1. Summary of observations

Observations were begun on 17 May, 1969, and ended on 28 May, 1969, with a five-day period, 19 to 24 May, during which no observations were made while FLIP was repositioned in the BOMEX array. Only a part of the available observations were selected for final interpretations. Observational data were not considered for final interpretations if adjustments described in the preceding section and applied on basis of preliminary analyses, were too extensive. In almost all cases, the periods that were rejected were those during which the wind direction was unfavorable with respect to the three sensor probes.

Those periods and observations selected for complete analyses and interpretations are listed in Table I. If it is considered that simultaneous measurements at two heights yield two sets of statistics, selected results represent 115 periods, each 10.9 min long.

4.2. Momentum-transfer results

Momentum-transfer results were examined primarily on the basis of the drag coefficient. As politely expressed by Holland (1972), the drag coefficient is not very useful for predicting stress from mean conditions, but it is valuable for comparing stress values and examining influences on momentum-transfer processes. Its value in the interpretation of data is that drag coefficients are intimately related to mean wind profiles which in turn are dependent on sensible heat transfer and, perhaps, wind-wave coupling by a relation of the form

$$C_{10} = \left[\frac{k}{\ln Z/Z_o - \Psi(Z/L,\, C/u_*)}\right]^2. \tag{2}$$

Z_o describes surface roughness, Z/L describes the stability effects where L is the Monin-Obukhov length, and C/u_* has been suggested by Volkov (1969, 1970) and Kitaigorodskii (1969) as a parameter for describing wind-wave coupling where C is the speed of the disturbing surface wave.

In this investigation, u_*, L and C were determined from covariance- and wave-spectra results as follows: $u_* = (-\overline{uw})^{1/2}$, $L = -\bar{T}u_*^3/(g \cdot 0.41 \cdot \overline{wT})$ and $C = g/2\pi n_o$ where n_o is the frequency of the wave spectrum peak. Furthermore, the propagation

TABLE I

Observational periods, levels and measurements

Period	Date May 1969	Inclusive times (GMT)	Level m	Parameters[a] measured	Number of[b] subperiods
1	17	2110–2230	6	1	7
„	17	2110–2230	3	1	7
2	19	0310–0430	6	2	7
„	19	0310–0430	2	2	7
3	19	0545–0700	6	2	7
4	19	1615–1730	8	2	6
5	19	1840–2000	6	2	7
„	19	1840–2000	3	2	2
6	19	2110–2150	8	2	3
7	24	2020–2130	8	1	4
8	26	1140–1200	8	2	2
9	26	1430–1455	8	2	2
10	26	1510–1545	8	2	3
11	26	1710–1730	8	2	2
12	26	2155–2240	8	2	4
13	27	0500–0545	8	2	4
14	27	0900–1020	8	2	6
15	27	1100–1215	8	2	6
16	27	1615–1735	8	2	6
„	27	1615–1735	3	2	4
17	28	0600–0612	8	2	1
18	28	0930–1050	8	2	4
19	28	1755–1915	3	2	6
20	28	2030–2145	8	2	6
				Total	115
				Total with all variables	96

[a] $1 \equiv u, v, w$.
$2 \equiv u, v, w, T$.
[b] 10.9 min long.

direction of the primary wave component which was the swell was observed to be in the same direction as U_{10}.

C_{10} is often related to the wind speed since the surface roughness, associated with Z_0, is expected to change with wind speed. C_{10}, as well as the u_* results as functions of U_{10}, appear in Figure 2. Wind speeds were adjusted to the 10-m level by assuming a neutral profile and using measured u_* and U_z values.

In Figure 2, C_{10} and u_* values are grouped over U_{10} intervals of 25 cm s^{-1} and plotted on against the average U_{10} value for the interval. Vertical and horizontal bars indicate standard deviations in each grouping. Regression analyses were performed on the grouped distributions. Regression coefficients appear in Table II. Results both unadjusted and adjusted, for the possible FLIP related contributions, are shown. Interpretation will apply to adjusted results since there appears to be no significant difference between adjusted and unadjusted results.

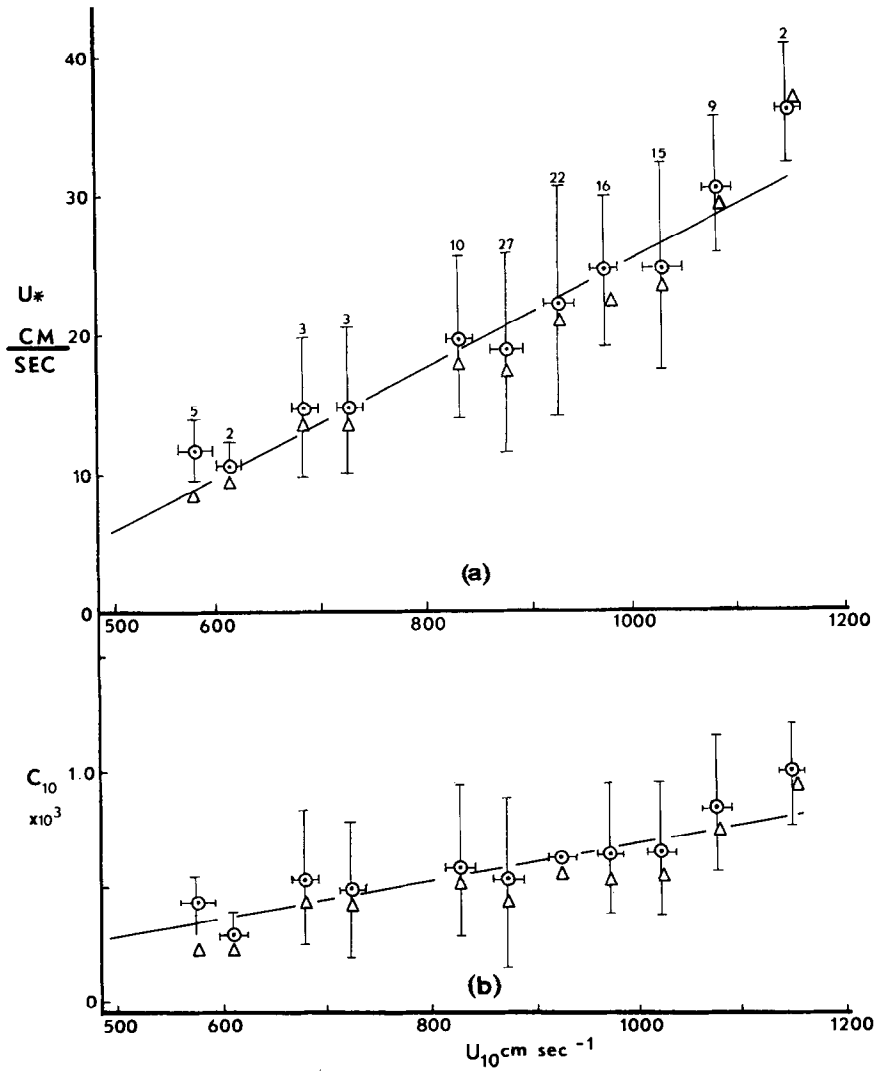

Fig. 2. Friction velocity (u_*) and drag coefficient (C_{10}) with respect to U_{10}, adjusted for possible FLIP motion, ○, and unadjusted △. Numbers of observations per grouped estimates are the same in (a) and (b). Straight lines correspond to regression results in Table II.

Three features are evident in the results. First, a zero intercept regression would not describe the u_* and U_{10} distributions; second, C_{10} values are much less than those reported by others in the BOMEX experiment; and third, there is a dependence of C_{10} on wind speed. The latter feature could be insignificant in view of the standard deviations of the mean estimates.

The relationship between u_* and U_{10} is interesting if one considers the linear regression equation (Table II) squared,

$$u_*^2 = 1.44 \times 10^{-3}\, U_{10}^2 - 0.50 U_{10} + 169. \tag{3}$$

TABLE II

Linear regression analyses results, based on distributions plotted in figures

(i) $y = ax + b$ $\qquad C/u_* = 88\ Z/L + 58$

	$x = U_{10}$ m s^{-1}						
y	a	b	rxy				
u_*	0.038 ± 0.004	-13.0	0.95				
$C_{10} \times 10^3$	0.83 ± 0.27	-15.0	0.71				
	$x = Z/L$			$x = C/u_*$			$C/u^* \propto a\ Z/L$
y	a	b	rxy	a	b	rxy	a
$-\psi(\ )$	40.0 ± 4.8	2.91	0.90	0.220 ± 0.012	-7.3	0.98	
σ_u/u_*	2.68 ± 1.12	2.43	0.70	0.022 ± 0.002	1.21	0.93	121
σ_v/u_*	2.27 ± 1.41	1.70	0.40	0.018 ± 0.004	1.08	0.74	126
σ_w/u_*	2.27 ± 0.60	1.20	0.79	0.018 ± 0.003	0.18	0.89	126

(ii) $\log y = a \log x + \log b$ or $y = bx^a$ $\qquad C/u_* = 129(Z/L)^{0.26}$

	$x = Z/L$			$x = C/u_*$			$C/u_* \propto (Z/L)^a$
y	a	b	$r \log x \log y$	a	b	$r \log x \log y$	a
C_{10}	-0.47 ± 0.21	0.241	0.82	-1.40 ± 0.10	257.0	0.93	0.32
σ_{T/T^*}	-0.28 ± 0.07	0.202	0.67	-0.61 ± 0.09	15.9	0.97	0.46
Ruw	-0.47 ± 0.10	0.093	0.87	-1.33 ± 0.94	70.8	0.94	0.36

On the basis of a discussion by Kitaigorodskii and Volkov, wherein the stress, τ, is separated into turbulent, τ_T, and wave related, τ_w, components, i.e.,

$$\tau = \tau_T + \tau_w, \tag{4}$$

we could view the first term in Equation (3) as being a component of the total stress which could be accounted for by a drag coefficient of 1.44×10^{-3}. Perhaps this component could correspond to τ_T. Interestingly, Cain (1971), from data observed at the same time, obtained a drag coefficient near 1.5×10^{-3} based on dissipation estimates of u_*. The dissipation method was specifically suggested by Volkov as a way to separate from the total stress the component associated with shear induced turbulence, τ_T. The other terms, $-0.50\ U_{10} + 169$, could be viewed as representing modifications to momentum transfer due to stability influence or the waves. In this expression it has a wind-speed dependence, which both stability and wind-wave coupling influences would have.

We conclude from the above interpretations and also from the standard deviations in C_{10} versus U_{10} results that the observed C_{10} results are not representable by a constant value nor are they functions only of wind speed. A possible C_{10} value excluding the wave and stability influences may have been 1.44×10^{-3}.

In comparison, Pond *et al.* (1971) reported a near constant value for C_{10}, approximately 1.5×10^{-3}. Furthermore, Pond *et al.* obtained similar values of C_{10} from dissipation- and eddy-correlation methods, 1.52 and 1.55 $\times 10^{-3}$, respectively, for C_8 which differs negligibly from C_{10}.

The influence of both the sensible heat transfer and the waves on the C_{10} results, as well as other statistics, will be examined on the basis of both unseparated and multiple relationships with Z/L and/or C/u_*. Such relationships for C_{10} appear in Figures 3 and 4. Except for magnitudes, there is little difference between C_{10} results which are adjusted or unadjusted for possible influence from FLIP's motion. Although a logarithmic representation of C_{10} vs Z/L is not completely valid, since C_{10} is defined at $Z/L = 0$, such a representation appears to describe both distributions equally well.

Two considerations in such an examination involving C/u_* and Z/L are (1) which parameter, u_* or C, determines the distributions of C/u_*, and (2) is the relationship between C/u_* and Z/L an important factor?

The joint frequency distribution for $1/u_*$ and C appears in Figure 5 along with the conditional mean of C/u_*. The greatest variations in C/u_* are associated with variations in u_* although for a given u_*, C/u_* varied from 1 to 2 standard deviations, $\sigma = 35$. Therefore, these values of C/u_*, which measure wind-wave coupling, will reflect changes in wave stages as well as u_* or wind speed.

With respect to the range of C/u_*, Volkov (1970) related C/u_* values to wave stages as follows: $C/u_* < 20$ as actively developing wave swell; $20 < C/u_* < 30 (U_{10} \approx C)$ as fully developed swell; and $C/u_* > 30$ as surge swell. Hence, most of these results fall into the surge swell category, but approach the fully developed swell category for which Volkov observed minimal wave influence on turbulence statistics. Therefore, one expects the results to include some with minimal or no wave influence.

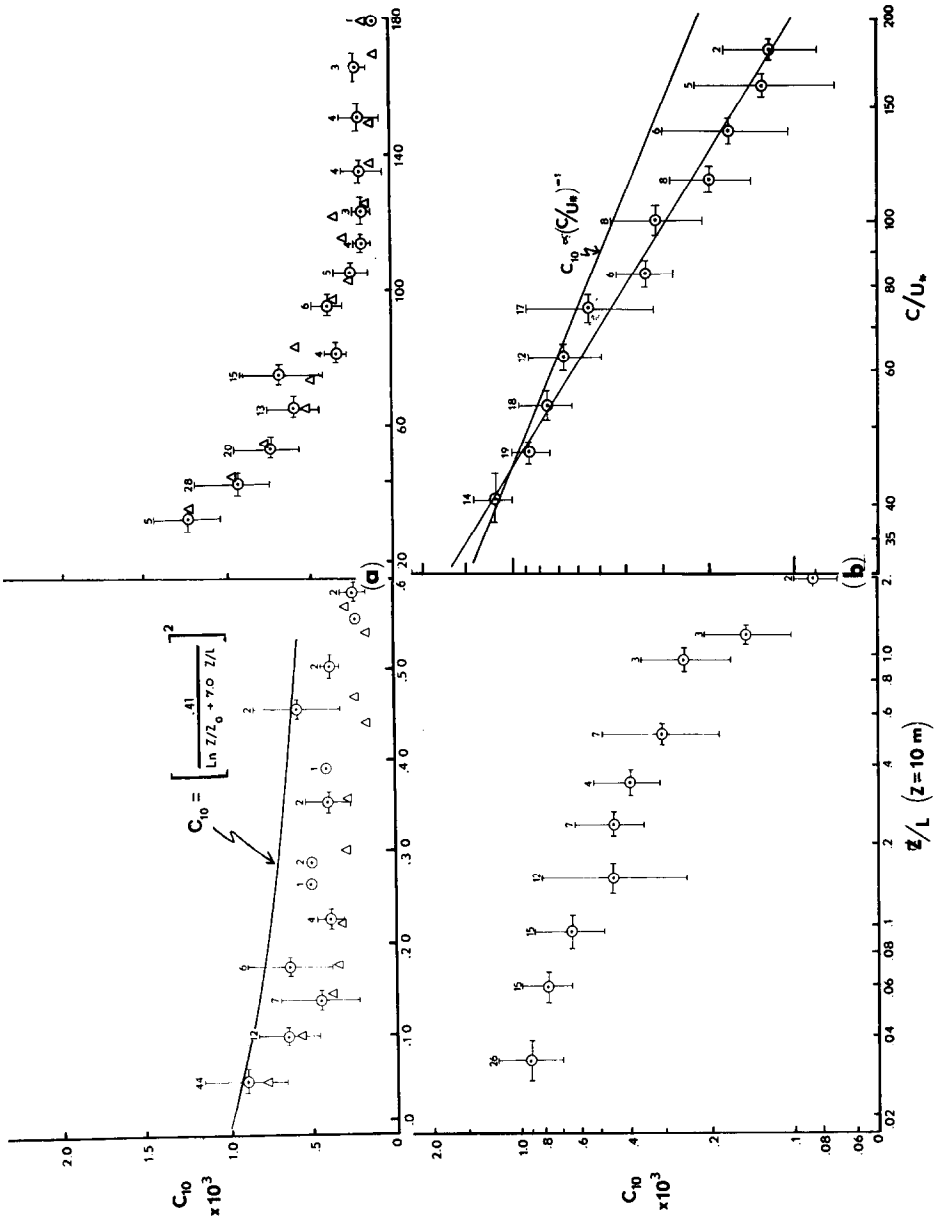

Fig. 3. C_{10} with respect to $Z/L(Z = 10\ m)$ and C/u^* for (a) linear and (b) logarithmic distributions. Adjusted for possible FLIP motion, ○, and unadjusted, Δ.

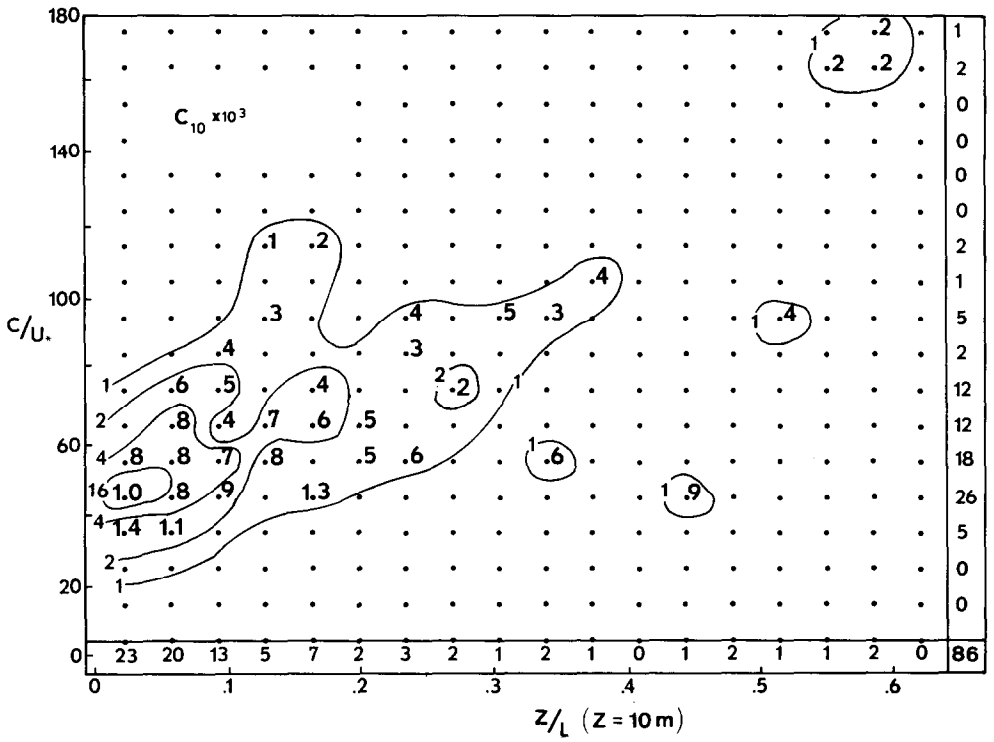

Fig. 4. Conditional mean (plotted numbers) of $C_{10} \times 10^3$ for joint-frequency distribution (delineated with solid labelled lines) of $C/u_*(Z = 10$ m) and Z/L. Integers along right and bottom edges are sums of occurrences in respective rows or columns. The total sum is 86 rather than 115, the number of periods available for examination, because either L was not available or values do not appear due to truncation of the Z/L range.

The relationship between Z/L and C/u_* is of interest because of the objective to identify, separately, influences of sensible heat flux and wind-wave coupling. A relationship between the two parameters is evident in the joint frequency distribution in Figure 4 and is further summarized in Figure 6.

In view of preceding discussion, C_{10} results in Figure 2 do appear to decrease in similar non-linear fashions with respect to both Z/L and C/u_*. From regression results in Table II we see that C_{10} relationships would require the exponential dependence between C/u_* and Z/L to be

$$\frac{C}{u_*} \alpha \left(\frac{Z}{L}\right)^{0.32}, \tag{5}$$

if the similarity of the distributions was due solely to the relationship between C/u_* and Z/L. In comparison, exponential regression analyses between C/u_* and Z/L yielded a 0.26 exponent on Z/L, Table II. Hence, separate influences on C_{10} by each of these parameters are probable.

Another difference in the two distributions is that C_{10} values are higher at the lower

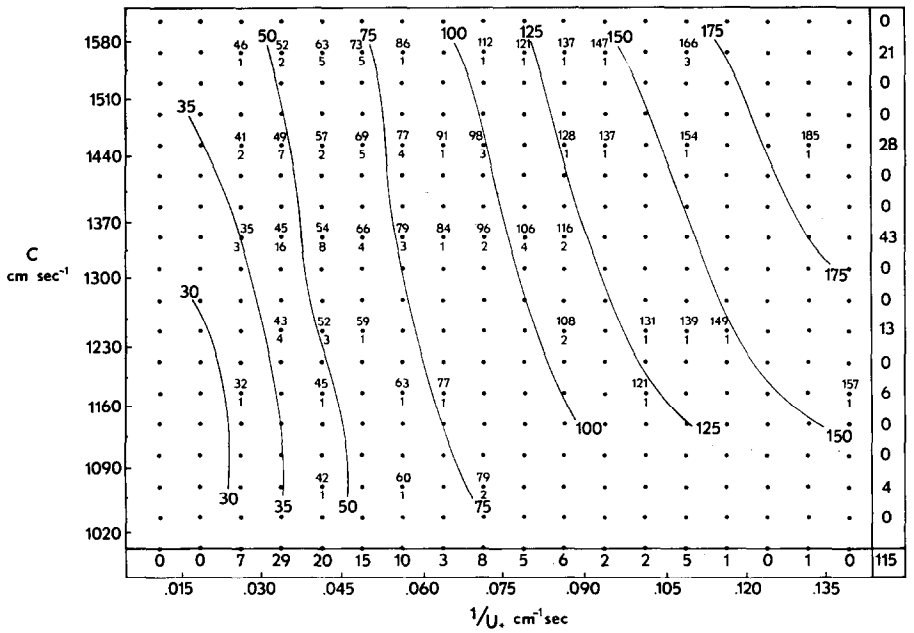

Fig. 5. Conditional mean (top number in cell) of C/u_* for joint-frequency distribution (bottom number in cell) of C and $1/u_*$. Solid labelled lines represent isolines of C/u_*.

C/u_* limit than at the lower Z/L limit. In Figure 3, C_{10} approaches 1.1×10^{-3} as Z/L approaches 0 and approaches 1.4×10^{-3} as C/u_* approaches 25. This difference is significant in view of the fact that, in the mean, low values of C/u_* are associated with low values of Z/L, Figure 6. It will be shown in the following discussion that C_{10} values of 1.4×10^{-3} also correspond to near-neutral Z/L values but only in association with C/u_* values near 30. In view of Volkov's findings, $C/u_* = 30$ could be associated with minimal wave influence conditions. Futhermore, it was noted that Cain (1971) obtained C_{10} values near 1.5×10^{-3} using the dissipation method which, according to Volkov, would not include the waves' influence in the estimate.

A final examination of the single, unseparated representations will be a comparison of the distributions in Figure 3 with possible predictions for C_{10} vs Z/L and C_{10} vs C/u_*. A prediction for C_{10} vs Z/L is given by Equation 2 after specification of the function $\Psi(Z/L)$. A frequently referenced specification is that by McVehil (1964), $\Psi(Z/L) = 7.0\ Z/L$. For the curve in Figure 3, this expression was used and Z_o was set equal to 0.0024 to make $C_{10} = 1.0 \times 10^{-3}$ at $Z/L = 0$. The results for C_{10} vs Z/L differ considerably from the prediction and suggest a possible influence due to the wind-wave coupling, C/u_*.

A possible prediction for C_{10} vs C/u_* could be one based on the observed linear relationships between C_{10} and U_{10} and between u_* and U_{10}. Such a prediction yields a $(C/U_*)^{-1}$ dependence for C_{10}. A comparison of the slope of the line computed from regression results in Table II with a -1 slope, Figure 3, indicates the prediction is not

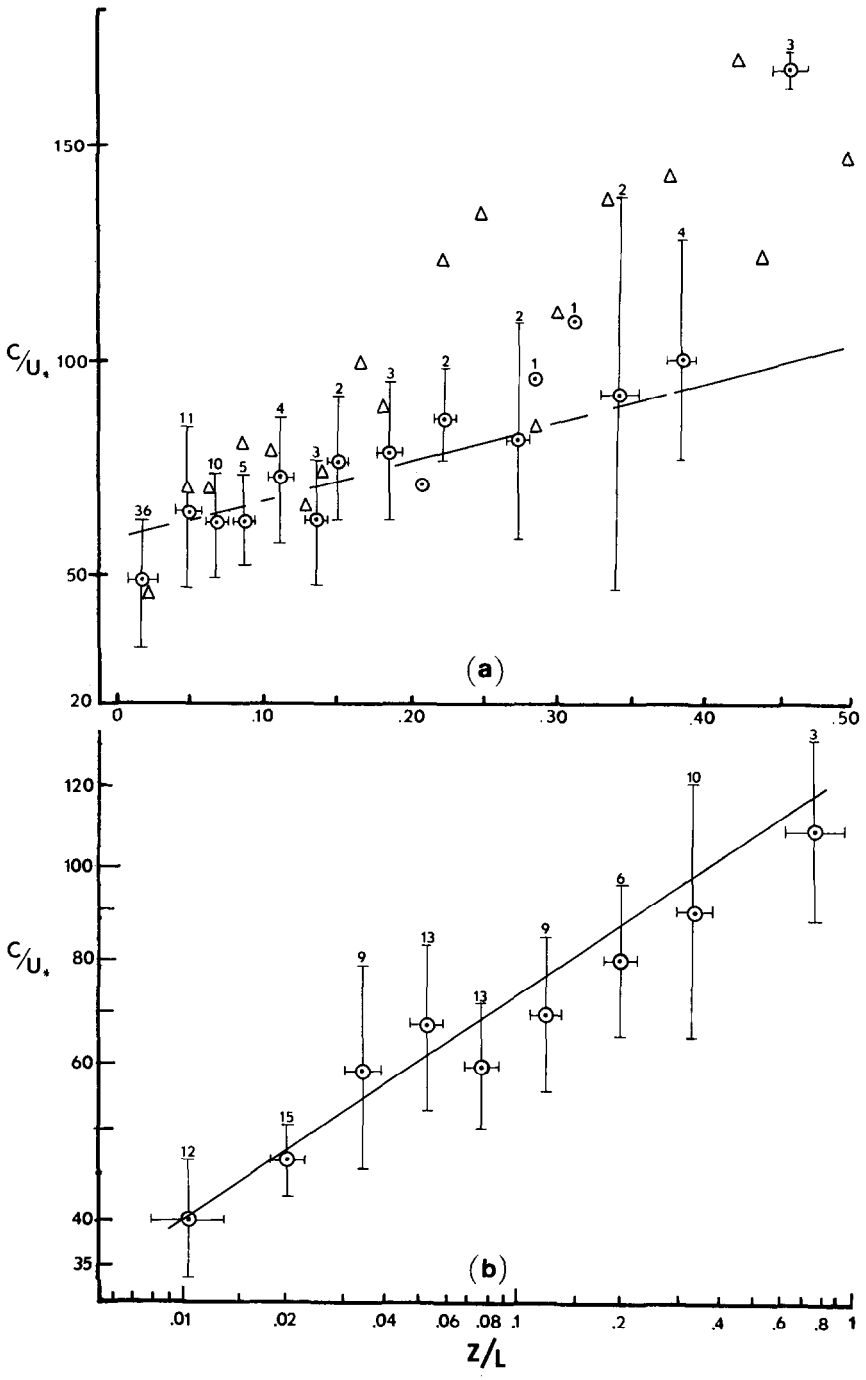

Fig. 6 C/u^* with respect to Z/L for (a) linear and (b) logarithmic distributions. Adjusted for possible FLIP motion, ○, and unadjusted, Δ.

accurate. The -1 slope line in Figure 3 was drawn to coincide with $C_{10}=1.4\times10^{-3}$ at $C/u_*=35$.

Preceding discussions on C_{10} have been more detailed with respect to single unseparated distributions than will be the case for other statistics. We conclude from it that the statistic C_{10} has separate dependences on Z/L and C/u_*. Without removing the dependence on C/u_*, C_{10} did not have the predicted dependence on Z/L for stable conditions. C_{10} did not change with C/u_* as predicted by linear relationships between C_{10} and U_{10} and u_* and U_{10}. Hence, U_{10} or Z_o are probably not sufficient parameters for describing the surface influcnce on the adjacent turbulent regime. Rather, a function of the form used in Equation (2), as proposed by Kitaigorodskii, may be required. We examine this possible dependence in the following discussions.

In Figure 4, C_{10} decreases with increases in both Z/L and C/u_*, one of which remaining constant. Also, C_{10} is approximately 1.4×10^{-3} for the joint distribution categories for $C/u_*\approx25$ and $Z/L=0$. Because of the limited distribution, however, one cannot judge if the change of C_{10} with respect to Z/L differs between high and low C/u_* values or vice versa, or if C_{10} decreases differently along the diagonal axis than along the horizontal or vertical axes. Therefore, the joint distribution will be summarized on the basis of multiple linear regression analyses.

The equation examined by regression analyses was the following, based on Equation (2), assuming that the C/u_* dependence has the same form as the dependence on Z/L, which is $\Psi(Z/L)=\alpha(Z/L)$,

$$0.41C_{10}^{-1/2}-\ln\frac{Z}{Z_0}=a\frac{Z}{L}+b\frac{C}{u_*}+c \tag{6}$$

where $Z=10$ m, $Z_o=0.024$ cm. The value $Z_o=0.024$ corresponds to the previously discussed value for C_{10}, i.e., 1.4×10^{-3}. The computed regression coefficients, Table III, yield the following form for Equation (6):

$$C_{10}=\left[\frac{0.41}{\ln\dfrac{Z}{Z_0}+6.44\dfrac{Z}{L}+0.13\left(\dfrac{C}{u_*}-26.3\right)}\right]^2,\ Z=10\text{ m}. \tag{7}$$

The above expression summarizes the C_{10} results with respect to Z/L and C/u_* and is quite remarkable. The dependence on Z/L is close to that observed by others; McVehil (1964), 7.0; Webb (1970), 5.2 and Businger *et al.* (1971), 4.7 with $K=0.35$. Also, when the constant from the regression results is incorporated into the C/u_* dependence, the wave influence is zero near a C/u_* value of 25, the value observed by Volkov (1969) for no wave influence.

The coefficient multiplying Z/L, 6.44, would have been different if Z/L values had been defined, as they should have been, by both sensible and latent heat transfer, Z/L_T and Z/L_q, respectively. Negative values are expected for Z/L_q over the sea so the net Z/L values were probably less than those yielding the regression coefficient in Equation (7). For the latter case, a favorable comparison on the basis of relative

TABLE III

Multiple linear regression analyses results, based on 96 observations

(i) $y = a \cdot Z/L + b \cdot C/u_* + c$				Partial correlations	
y	a	b	c	$r_{y \cdot \frac{Z}{L}}$	$r_{y \cdot \frac{C}{u_*}}$
$(.41\ C_{10}^{-1/2}$					
$-\ln Z/Z_o)$	6.44 ± 0.71	0.126 ± 0.013	-3.55	0.87	0.94
$-\Psi(\ )$	6.57 ± 1.00	0.162 ± 0.013	-4.21	0.79	0.93
σ_u/u_*	0.34 ± 0.20	0.023 ± 0.002	1.21	0.62	0.80
σ_v/u_*	1.33 ± 0.19	0.005 ± 0.002	1.58	0.77	0.78
σ_w/u_*	0.69 ± 0.10	0.014 ± 0.001	0.47	0.72	0.82

(ii) $\log y = a \log Z/L + b \log C/u_* + \log c$ or $y = c(Z/L)^a \cdot (C/u_*)^b$					
y	a	b	c	$r_{\log \frac{Z}{L} \log y}$	$r_{\log \frac{C}{u_*} \log y}$
C_{10}	-0.15 ± 0.05	-1.260 ± 0.161	220.0	0.79	0.92
σ_T	-0.27 ± 0.04	0.100 ± 0.120	0.60	0.77	0.77
Ruw	-0.15 ± 0.06	-1.020 ± 0.187	120.0	0.75	0.82

magnitudes can be made with McVehil's observed coefficient, $\alpha = 7.0$. The disadvantage in not having humidity data is certainly quite evident in these interpretations of Equation (7).

To examine further the assumed dependence on C/u_* without introducing possible errors due to adjustments to the 10-m level, $-\Psi(Z/L, C/u_*)$ was computed from the u_*, U_z and Z values as follows

$$-\Psi(Z/L, C/u_*) = -\ln \frac{Z}{Z_o} + 0.41 \frac{U_z}{u_*}, \tag{8}$$

with $Z_o = 0.024$. These results appear in Figures 7 and 8. From preceding discussion, we can state that distributions in Figure 7 do not reflect the separate dependencies. However, linear relationships appear to be appropriate for both distributions over the entire Z/L range and for C/u_* up to 140.

Joint frequency-conditional mean results in Figure 8 appear to support an assumed linear dependence on C/u_*. At least, such a limited distribution does not indicate that the relationship for C/u_* should be different than that for Z/L, which is expected to be linear.

Multiple linear regression results for the expression

$$-\Psi(Z/L, C/u_*) = a \frac{Z}{L} + b \frac{C}{u_*} + c \tag{9}$$

appear in Table III. The coefficients yield the following from Equation (9)

$$-\Psi(Z/L, C/u_*) = 6.57 \frac{Z}{L} + 0.16 \left(\frac{C}{u_*} - 26.3 \right) \tag{10}$$

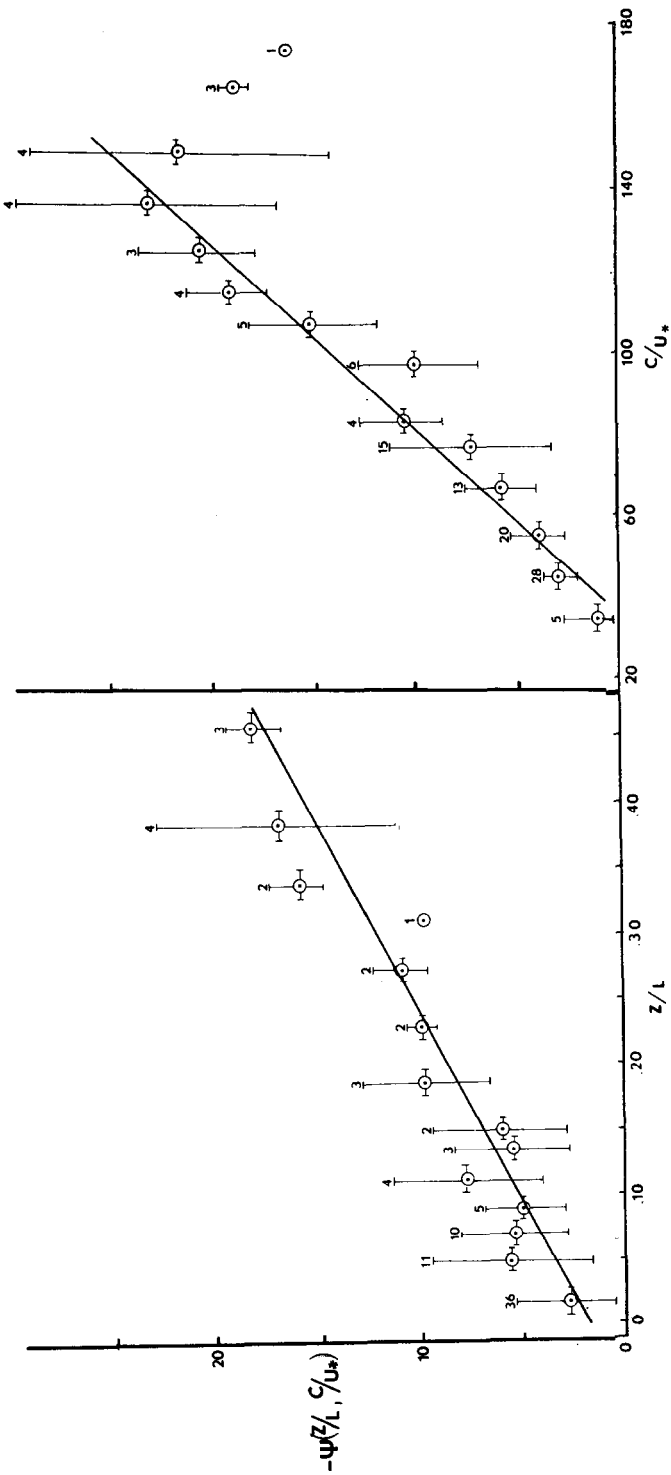

Fig. 7. Logarithmic profile deviation, $-\Psi(Z/L, C/u_*)$ from Equation (9), with respect to Z/L and C/u_*.

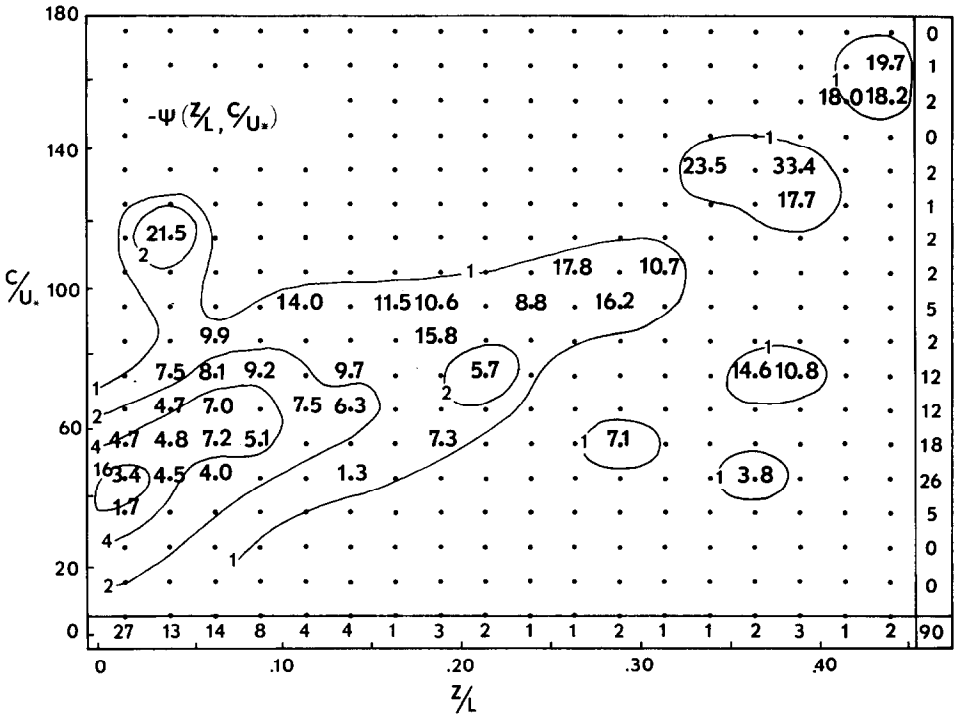

Fig. 8. Conditional mean of $-\Psi(Z/L, C/u_*)$ computed from Equation (9). Format same as in Figure 4.

which is nearly identical to the expression obtained from the C_{10} results. A similarity between the expressions was expected because the latter computations are identical to those for C_{10} except that U_z and Z/L are not adjusted to 10 m.

Equation (10), or (7), represents the expressed purpose of the investigation, with regard to momentum transfer results, since it describes the separate influences of hydrostatic stability and wind-wave coupling on the observed turbulence. Its appropriateness in this regard is based primarily on the agreement with results for the stability dependence and with results of Volkov for which $C/u_* = 25$ corresponded to minimal wind-wave coupling influence and for which $C/u_* > 25$ corresponded to reduced momentum transfer, in comparison to that expected for neutral conditions.

Concern about the appropriateness of Equation (10) is primarily associated with the data available for its formulation. The distribution of Z/L and C/u_* results hindered closer examination of the assumed linear relationship for C/u_*. Joint frequency-conditional mean distributions were specifically displayed to show this aspect of the data. Higher order terms or terms involving the products of Z/L and C/u_* are, perhaps, required and a better distribution would allow examination of this. The height dependence of the C/u_* term could not be examined, since almost all of the results were from one level, 8m. Not having moisture flux data was certainly an unfavorable aspect.

4.3. Relative intensity of fluctuations

Statistics on turbulent fluctuations defined by relative intensities have been related to both Z/L, e.g., Monin (1962), McBean (1971), and to C/u_* by Volkov (1969). Relative intensities considered are σ_u/u_*, σ_v/u_*, σ_w/u_* and σ_T/T_*. A dependence of σ_u/u_* and σ_w/u_* on Z/L or C/u_* also leads to a dependence for the correlation coefficient, $Ruw = -\overline{uw}/\sigma_u\sigma_w$.

Relations for these statistics with respect to Z/L are not as certain as those for C_{10} and associated profile predictions with respect to Z/L. Results from stable conditions are especially small in number. Therefore, the interpretations will be based to a large extent on the physical consistencies noted in the C_{10} and $\Psi(Z/L, C/u_*)$ results. We consider, for example, $C/u_* = 25$ as an approximate value associated with minimal wave influence on the statistics.

Single distributions, which have been shown to be poor representations of the normalized velocities, appear in Figure 9. They are presented here for comparison with the results of others. The largest differences between unadjusted and adjusted results, for possible FLIP motion influence, occur for these statistics. The difference is most pronounced in the Z/L distributions especially for σ_u/u_*. Such large differences are expected because the standard deviations were always decreased, an average of 8%, and the u_* estimates were generally increased, an average of 8%, by the adjustments.

In comparison with results of others, Volkov observed greater increases of σ_u/u_* and σ_w/u_* with respect to C/u_*. Deleonibus (1971) observed a linear increase for σ_w/u_* which was nearly identical to these results, 0.019 C/u_* vs 0.018 C/u_*, but his σ_w/u_* values were greater. Deleonibus' σ_w/u_* values also increased with increasing stability although he did not interpret the trend to be significant. Linear trends of these statistics with respect to Z/L were also evident in over-land results of McBean (1971). However, he questioned the results for stable conditions due to uncertainties in the data.

Joint frequency-conditional mean distributions for σ_u/u_*, σ_v/u_* and σ_w/u_* appear in Figure 10. For joint-distribution categories for which $C/u_* \cong 25$ and $Z/L = 0$, σ_u/u_*, σ_v/u_* and σ_w/u_* values are near 2.3, 1.9, and 1.1, respectively. Values reported by others for near-neutral conditions over land appear in Table IV. In view of the preceding interpretations, neutral-over land values should approximate those for which $C/u_* \approx 25$ and $Z/L = 0$. The values of σ_u/u_* and σ_w/u_* coincide with those reported by Volkov (1969) and the value of σ_v/u_* coincides with that reported by McBean (1971). Pond, *et al.* (1971) observed a mean σ_w/u_* value of 1.32 for 20 periods for which Z/L was near -0.2.

Multi-linear regression analysis results, from adjusted values, in Table III yield the following expressions, written so the wave influence is zero at $C/u_* = 26.3$,

$$\begin{aligned}
\sigma_u/u_* &= 0.34\ Z/L + 0.023\ (C/u_* - 26.3) + 1.81 \\
\sigma_u/u_* &= 1.33\ Z/L + 0.005\ (C/u_* - 26.3) + 1.71 \\
\sigma_w/u_* &= 0.69\ Z/L + 0.014\ (C/u_* - 26.3) + 0.84.
\end{aligned} \tag{11}$$

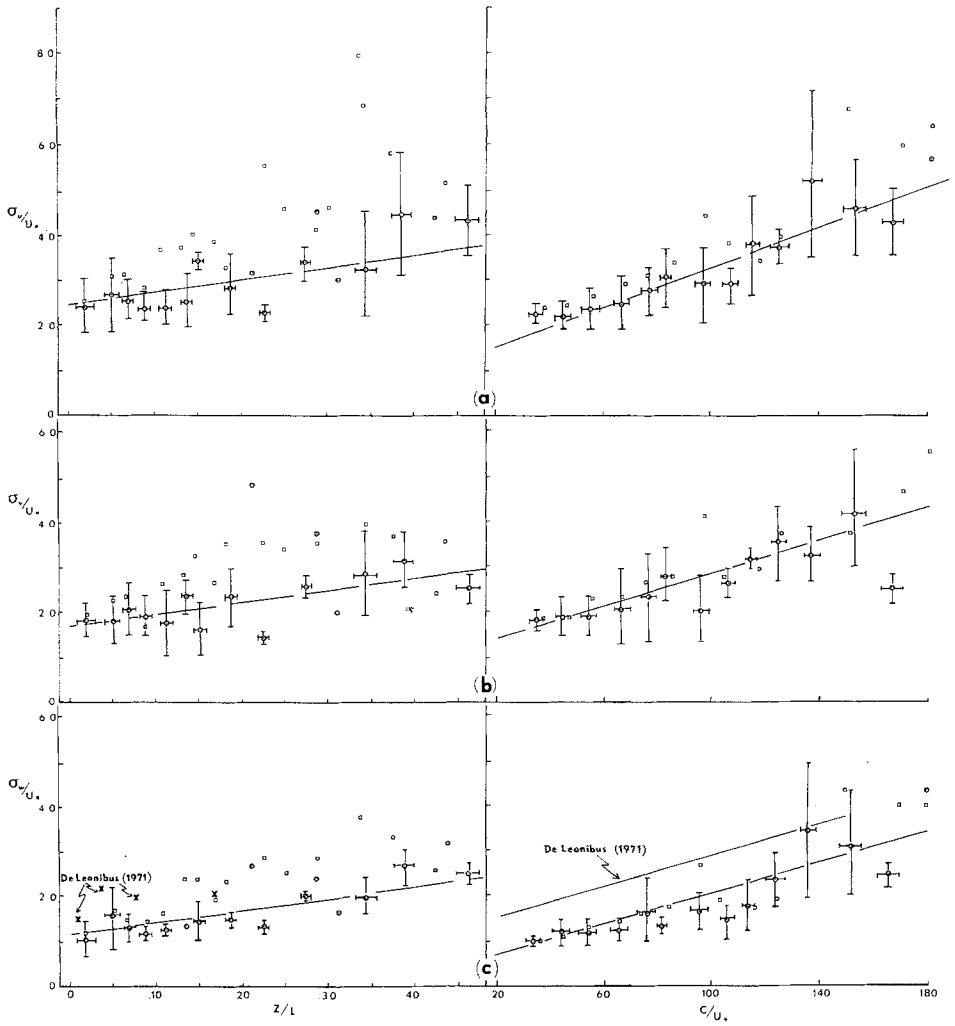

Fig. 9. Relative intensities of velocity fluctuations, (a) σ_u/u_*, (b) σ_v/u_* and (c) σ_w/u_* with respect to Z/L and C/u_*. Distribution of observations same as in Figure 6 for Z/L and Figure 3 for C/u^*. Adjusted, ○, and unadjusted, □, results

TABLE IV

Relative intensities suggested for near-neutral conditions over land

Reference	σ_u/u_*	σ_v/u_*	σ_w/u_*
McBean (1971)	2.2	1.9	1.4
Volkov (1969)	2.3	–	1.2
Prasad and Panofsky (1967)	2.5	2.0	1.3

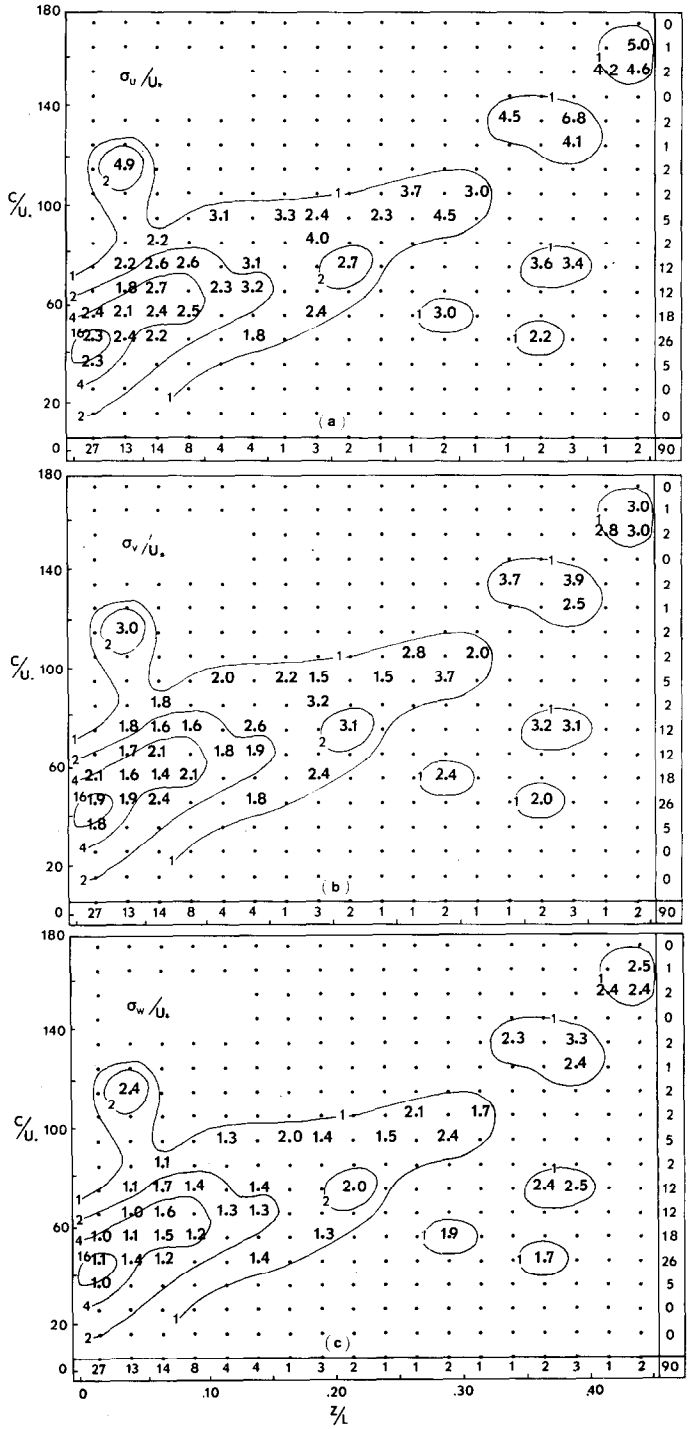

Fig. 10. Conditional mean of (a) σ_u/u_*, (b) σ_v/u_*, and (c) σ_p/u_* for joint frequency distribution of C/u_* and Z/L. Format same as in Figure 4.

Regression results at $Z/L=0$ and C/u_* near 25 do not agree with those appearing in the joint frequency-conditional mean distributions. A possible reason for this could be the large values occurring above $C/u_*=130$, which was also an anomalous region in the $-\Psi(Z/L, C/u_*)$ vs C/u_* distributions. However, removing observations with $C/u_*>130$ from the regression computations did not improve the agreement. This result may suggest a possible non-linear form for the dependencies, especially the C/u_* dependence.

We note that in the multiple-regression results, trends of σ_u/u_* and σ_w/u_* with respect to Z/L change considerably between the single and multiple regressions but change very little with respect to C/u_*. The dependence of σ_v/u_* on C/u_* is observed to be less than that of σ_u/u_* or σ_w/u_*. This is attributable to the fact that the disturbing waves propagated in the general direction of the mean wind and, therefore, influences on σ_v/u_* were not so consistent.

As was the case for momentum transfer, Equation (11) represents the purpose of the investigation with regard to turbulent fluctuations. It describes the separate influences of stability and wind-wave coupling on the statistics, relative intensities. Its appropriateness is based primarily on the fact that for $Z/L=0$ and C/u_* near 25 the respective values are in agreement with those observed during neutral conditions over land. This agreement is best observed from the examination of joint frequency-conditional mean distributions. Regression results, summarized in Equation (11), predict these values within acceptable ranges.

Unfavorable considerations for these statistics are similar to those for C_{10} and $-\Psi(Z/L, C/u_*)$ except that an expected dependence for Z/L was not as certain. Confidence in the Z/L dependence was important in interpreting the momentum transfer results.

The statistic *Ruw* is of interest because of its use in recent analyses of over-water data for adjustments to possible probe alignment errors, Pond *et al.* (1971). A value near -0.5 for low frequencies was assumed in such adjustments. *Ruw* is known to have a stability dependence but a possible dependence on the waves' influence, C/u_*, will be sought in our interpretation. The dependence of *Ruw* on Z/L and C/u_* could be formulated from regression expressions for σ_u/u_* and σ_w/u_* since the inverse of their product would be the predicted relation. Such an expression was not examined from the regression results. Rather, the distribution in Figure 11 is examined. The $-Ruw$ value corresponding to the lowest $C/u_*-Z/L$ joint frequency interval is, in fact, 0.5 but decreases in $-Ruw$ are quite evident for increases in both Z/L and C/u_*.

The final fluctuation statistic considered is σ_T/T_*. A significant result for this statistic is that its dependence on C/u_* is opposite, increasing, from its dependence on Z/L, decreasing. This feature is identifiable only in the conditional mean (Figure 12) and multiple-regression results (Table III). Such a result differs from the relationships observed by Volkov (1969) who observed σ_T/T_* to decrease with increasing C/u_*. However, the greatest decrease in Volkov's results occurred below $C/u_*=25$. Over the range corresponding to our data, his σ_T/T_* values exhibited very little, if any, change.

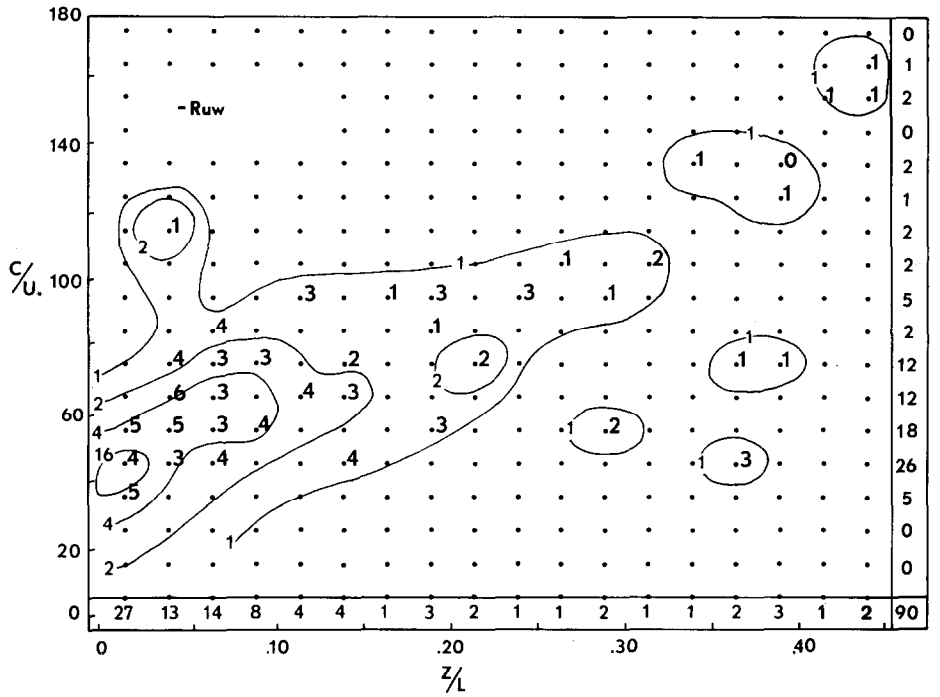

Fig. 11. Conditional mean of $-Ruw$ for joint frequency distribution of C/u_* and Z/L. Format same as in Figure 4.

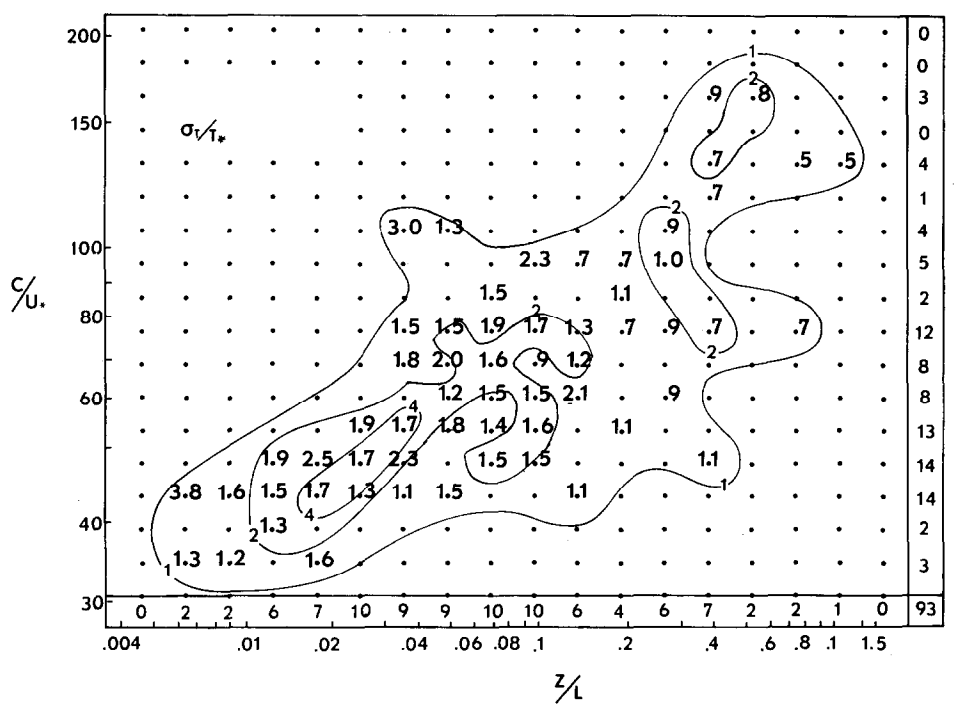

Fig. 12. Conditional mean of σ_T/T_* for joint frequency distribution of ln C/u_* and ln Z/L. Format same as in Figure 4.

Conditional mean results in Figure 12, shown for logarithmic distributions of Z/L and C/u_*, reflect the multiple regression results. As Z/L increases, σ_T/T_* decreases and as C/u_* increases, σ_T/T_* increases. The dependence on C/u_* appears to be different for near-neutral conditions, $Z/L<0.1$, where it increases. Regression results in Table III reflect this uncertainty in the C/u_* trend since the standard deviation of the exponent indicates that it could be either positive or negative.

5. Summary and Conclusions

The purpose of this investigation is to describe observational results on momentum and sensible heat transfer and intensities of turbulent fluctuations measured above ocean waves. A primary objective in the interpretations is to identify separate influences of stability and windwave coupling. Several aspects of the observational and analysis procedures were presented because the data were obtained on a platform which was not completely steady and also because there were inherent difficulties in analyzing the turbulence data.

Momentum-transfer results, based on the drag coefficient, revealed an influence by wind-wave coupling as well as stability. A possible C_{10} value, with stability and wind-wave coupling influences removed, was identified to be 1.4×10^{-3}. Possible successful separation of the influence of stability, Z/L, and wind-wave coupling, C/u_*, on C_{10} is concluded on the basis of agreement with over-land empirical relationships for stable conditions depending on Z/L and agreement with Volkov's observation that near $C/u_*\cong25$ the wind-wave coupling influence should be minimal. The effect of wind-wave coupling for $C/u_*>25$ was the same as that observed by Volkov. Its influence was to decrease the momentum transfer from that associated with a neutral wind profile. Therefore, the influence of wind-wave coupling for $C/u_*>25$ was observed to have the same effect as the influence of hydrostatic stability during stable conditions.

A significant result from the examination of the relative intensities (for σ_u/u_*, σ_v/u_* and σ_w/u_*) was that for joint intervals near $Z/L=0$ and $C/u_*=25$, conditional mean values of σ_u/u_*, σ_v/v_* and σ_w/u_* were all in good agreement with those values suggested for neutral conditions over land. Multi-linear regression results yielded expressions which predict the neutral over-land values within 20, 10 and 25, per cent for σ_u/u_*, σ_v/u_* and σ_w/u_*, respectively, for $Z/L=0$ and $C/u_*=26.3$. A C/u_* value of 26.3 was observed in momentum-transfer results to be associated with no wind-wave coupling influence.

With respect to the $-Ruw$ results, near $Z/L=0$ and $C/u_*\approx25$ $-Ruw$ had the expected 0.5 value. $-Ruw$ was observed to decrease with increasing C/u_* which was a relation also noted by Volkov (1970).

σ_T/T_* results did not show the dependence on C/u_* observed by Volkov (1969). This was most likely due to the fact that the C/u_* range for these data did not correspond to the range, $C/u_*<25$, where Volkov noted the largest effect.

These interpretations of momentum-transfer and fluctuation statistics have described the separate influences of stability and wind-wave coupling. Regression results

indicated that for these observations the waves' influence was as significant as the stability influence in causing deviations from results during neutral conditions over land. The interpretations required considerable comparison with previous results for stable conditions and wind-wave conditions, defined by C/u_*. These results agreed with the separate influences as described by others, especially Volkov and Kitaigorodskii.

Additional investigations of this kind are strongly advocated due to limitations imposed by the data used in this one. These limitations were the lack of humidity data, the range of C/u_* and Z/L values and the fact that the height dependence of the C/u_* influence was not examined.

Acknowledgements

The author is very grateful to persons at the University of Michigan who participated in the collection and analyses of the data. Particular thanks, are extended to Mr Michael Walter for significant contributions in data reduction, analyses and preliminary interpretation of the results. Dr D. J. Portman, and Mr Allen Davis were also involved in all aspects of the experimental design, measurements and analyses. The author also wishes to thank Messrs. Steve Rinard and David Norman of the Naval Postgraduate School for assistance in completing computer computations.

The study was performed with support from the Office of Naval Research, under Contract Number N00014-67-A-0181-0005 with the University of Michigan and NR083265 with the Naval Postgraduate School and with support from the Naval Ordnance Systems Command, Account NR 56657 at the Naval Postgraduate School.

References

Businger, J. A., Wyngaard, J. C., Izumi, W., and Bradley, E. F.: 1971, 'Flux-Profile Relationships in the Atmospheric Surface Layer', *J. Atmospheric Sci.* **28**, 181–189.

Cain, J. D.: 1971, 'A Comparison of Momentum Fluxes Determined from Time and Space Structure Functions', M. S. Thesis, Texas A and M Univ.

DeLeonibus, P. S.: 1971, 'Momentum Flux and Wave Spectra Observations from Sea Surface Evaporation, Energy Flux and Ocean Tower', *J. Geophys. Res.* **76**, 6505–6527.

Holland, J. Z.: 1972, 'Comparative Evaluation of Some BOMEX Measurements of Sea Surface Evaporation, Energy Flux and Stress', *J. Phys. Oceanog.* **2**, 476–486.

Kitaigorodskii, S. A.: 1969, 'Small Scale Atmosphere-Ocean Interactions', *Izv. Atmospheric and Oceanic Phys.* **5**, 641–649.

McBean, G. A.: 1971, 'The Varaiation of the Statistics of Wind, Temperature and Humidity Fluctuations with Stability', *Boundary-Layer Meteorology* **61**, 438–457.

McVehil, G. E.: 1964, 'Wind and Temperature Profiles near the Ground in Stable Stratification', *Quart. J. Roy. Meteorol. Soc.* **90**, 136–146.

Mollo-Christensen, E.: 1968, 'Wind Tunnel Test of the Superstructure of the *R/V* FLIP for Assessment of wind Field Distortoin', Report 68–2, Fluid Dynamics Lab., M.I.T., 29 pp.

Monin, A. S.: 1962, 'Empirical Data on Turbulence in the Surface Layer of the Atmosphere', *J. Geophys. Res.* **67**, 3103–3109.

Oort, A. H. and Taylor, A.: 1969, 'On the Kinetic Energy Spectrum near the Ground', *Monthly Weather Rev.* **97**, 623–636.

Paulson, C. A., Leavitt, E., and Fleagle, R. G.: 1972, 'Air-Sea Transfer of Momentum, Heat and

Water Determined from Profile Measurements During BOMEX', *J. Phys. Oceanog.* **2**, 437–447.
Pond, S., Phelps, G. T., Paquin, J. E., McBean, G., and Stewart, R. S.: 1971, 'Measurements of the Turbulent Fluxes of Momentum, Moisture and Sensible Heat over the Ocean', *J. Atmospheric Sci.* **28**, 901–917.
Prasad, B. and Panofsky, H. A.: 1967, 'Properties of Variances of the Meteorological Variables at Round Hill', R and D Technical Report ECOM-0035-F, Final Report from the Pennsylvania State University, August 1967, 65–93.
Superior, W. J.: 1969, 'BOMEX Flux and Profile Measurements from FLIP', Final report: Contract N62306-69-c-0186, for U.S. Naval Oceanographic Office, C. T. Thornthwaite Associates Laboratory of Climatology, 32 pp.
Volkov, Y. A.: 1969, 'The Spectra of Velocity and Temperature Fluctuations in Airflow Above the Agitated Sea Surface', *Izv. Atmospheric and Oceanic Phys.* **5**, 723–730.
Volkov, Y. A.: 1970, 'Turbulent Flux of Momentum and Heat in the Atmospheric Surface Layer over Disturbed Sea Surface', *Izv. Atmospheric and Oceanic Phys.* **6**, 770–774.
Webb, E. K.: 1970, 'Profile Relationships: The Log-Linear Range, and Extension to Strong Stability', *Quart. J. Roy. Meteorol. Soc.* **96**, 67–90.